Molecular Plant
Research article

CellPress
Partner Journal

Distinctive and complementary roles of E2F transcription factors during plant replication stress responses

Maherun Nisa[1,2,5], Thomas Eekhout[3,4], Clara Bergis[1,2], Jose-Antonio Pedroza-Garcia[3,4], Xiaoning He[1,2], Christelle Mazubert[1,2], Ilse Vercauteren[3,4], Toon Cools[3,4], Rim Brik-Chaouche[1,2], Jeannine Drouin-Wahbi[1,2], Layla Chmaiss[1,2], David Latrasse[1,2], Catherine Bergounioux[1,2], Klaas Vandepoele[3,4], Moussa Benhamed[1,2], Lieven De Veylder[3,4,6] and Cécile Raynaud[1,2,6,*]

[1]Université Paris-Saclay, CNRS, INRAE, Université Evry, Institute of Plant Sciences Paris-Saclay (IPS2), 91190 Gif-sur-Yvette, France

[2]Université de Paris Cité, CNRS, INRAE, Institute of Plant Sciences Paris-Saclay (IPS2), 91190 Gif-sur-Yvette, France

[3]Department of Plant Biotechnology and Bioinformatics, Ghent University, 9052 Ghent, Belgium

[4]Center for Plant Systems Biology, VIB, 9052 Ghent, Belgium

[5]Present address: Plant Molecular and Cellular Biology Laboratory, Salk Institute for Biological Studies, La Jolla, CA 92037, USA

[6]Senior author

***Correspondence: Cécile Raynaud (cecile.raynaud@universite-paris-saclay.fr)**

https://doi.org/10.1016/j.molp.2023.07.002

ABSTRACT

Survival of living organisms is fully dependent on their maintenance of genome integrity, being permanently threatened by replication stress in proliferating cells. Although the plant DNA damage response (DDR) regulator SOG1 has been demonstrated to cope with replication defects, accumulating evidence points to other pathways functioning independent of SOG1. Here, we report the roles of the *Arabidopsis* E2FA and EF2B transcription factors, two well-characterized regulators of DNA replication, in plant response to replication stress. Through a combination of reverse genetics and chromatin immunoprecipitation approaches, we show that E2FA and E2FB share many target genes with SOG1, providing evidence for their involvement in the DDR. Analysis of double- and triple-mutant combinations revealed that E2FB, rather than E2FA, plays the most prominent role in sustaining plant growth in the presence of replication defects, either operating antagonistically or synergistically with SOG1. Conversely, SOG1 aids in overcoming the replication defects of E2FA/E2FB-deficient plants. Collectively, our data reveal a complex transcriptional network controlling the replication stress response in which E2Fs and SOG1 act as key regulatory factors.

Key words: replication stress, E2F, SOG1, cell cycle, *Arabidopsis*

Nisa M., Eekhout T., Bergis C., Pedroza-Garcia J.-A., He X., Mazubert C., Vercauteren I., Cools T., Brik-Chaouche R., Drouin-Wahbi J., Chmaiss L., Latrasse D., Bergounioux C., Vandepoele K., Benhamed M., De Veylder L., and Raynaud C. (2023). Distinctive and complementary roles of E2F transcription factors during plant replication stress responses. Mol. Plant. **16**, 1269–1282.

INTRODUCTION

In all eukaryotic organisms, faithful transmission of genetic information from one generation to the next strongly depends on accurate DNA replication. Several factors, including pyrimidine dimers, unrepaired DNA lesions, RNA–DNA hybrids, and formation of DNA secondary structures, can disrupt or slow down DNA replication. These factors can result in fork stalling, leading to replication stress that may, in turn, affect genomic integrity (Mazouzi et al., 2014). Because of the multiplicity of factors that can lead to fork stalling, replication stress is a ubiquitous threat to the maintenance of genome integrity in all proliferating cells. Interestingly, in plants, there is accumulating evidence that exposure to abiotic or biotic stresses can trigger the DNA

Published by the Molecular Plant Shanghai Editorial Office in association with Cell Press, an imprint of Elsevier Inc., on behalf of CSPB and CEMPS, CAS.

damage response (DDR) (Nisa et al., 2019; Pedroza-Garcia et al., 2022), and this effect could partly be due to increased replication stress (Nisa et al., 2021).

In eukaryotes, the DDR signaling cascade is largely conserved and activates checkpoints that induce cell cycle arrest until the damaged DNA is repaired. The DDR is activated by DNA double-strand breaks (DSBs) or replication stress and relies on the two protein kinases ATAXIA TELANGIECTASIA MUTATED (ATM) and ATM AND RAD3- RELATED (ATR), respectively (Maréchal and Zou, 2013). In animal and yeast cells, when the progression of DNA replicative polymerases is hindered, REPLICATION PROTEIN A-coated single-stranded DNA accumulates, resulting in recruitment and activation of ATR (Saldivar et al., 2017) through mechanisms that appear to be conserved in plants (Sweeney et al., 2009). By contrast, downstream signaling events differ between plants and animals. In plants, ATR is thought to directly phosphorylate the central DDR transcriptional regulator SUPPRESSOR OF GAMMA-RESPONSE 1 (SOG1), which, in turn, activates DNA repair genes and negative regulators of cell cycle progression, such as WEE1 (Preuss and Britt, 2003; De Schutter et al., 2007; Sjogren et al., 2015; Bourbousse et al., 2018). However, when treated with hydroxyurea (HU), which triggers replication stress by depleting the intracellular desoxyribonucleotides pool, *wee1 sog1* double mutants display stronger growth inhibition than the corresponding single mutants, indicating that SOG1 and WEE1 function partially independently to control the replication stress response (Hu et al., 2015). Likewise, hypomorphic mutants of the replicative DNA polymerase ε (Polε) catalytic subunit POL2A show constitutive activation of the replication stress response that is only partially dependent on SOG1. Indeed, ATR and WEE1 are crucial for the survival of *pol2a*, but the *pol2a sog1* double mutant is viable and still shows activation of a subset of DDR genes (Pedroza-Garcia et al., 2017), indicating that part of the transcriptional response evoked by replication stress is controlled by a still unidentified transcription factor.

Given their role as transcriptional activators of genes required for S phase progression, possible contributors to the transcriptional reprograming induced by replication stress could be E2F transcription factors. Among other functions, the E2F–RBR1 (RETINOBLASTOMA-RELATED 1) module plays a well-known role in control of DNA replication (Müller et al., 2001; Vlieghe et al., 2003; Vandepoele et al., 2005; Naouar et al., 2009). When a plant cell receives mitogenic cues, D-type, cyclin-activated, cyclin-dependent kinases phosphorylate RBR1, which unleashes E2F activity. In *Arabidopsis*, the E2F family comprises six members: E2FA, E2FB, E2FC, DEL1/E2Fe, DEL2/E2Fd, and DEL3/E2Ff (Vandepoele et al., 2002). They are categorized into canonical E2Fs (E2FA, E2FB, and E2FC), which function as heterodimers with their dimerization partners DPA and DPB, and non-canonical E2Fs (DEL1/E2Fe, DEL2/E2Fd, and DEL3/E2Ff), which operate independent of dimerization partners (Mariconti et al., 2002; Lammens et al., 2009). Canonical E2FA and E2FB are considered transcriptional activators because they contain a transactivation domain and stimulate S phase entry, whereas E2FC is generally considered a repressor (De Veylder et al., 2002; del Pozo et al., 2002; Mariconti et al., 2002; Sozzani et al., 2006; Lammens et al., 2009). E2FA and E2FB are thought to be partially redundant because single mutants of *E2FA* and *E2FB* show no dramatic phenotypes (Yao et al., 2018; Őszi et al., 2020), whereas a double mutant is lethal (Li et al., 2017). However, some differences exist between E2FA and E2FB. For example, E2FA and E2FB play different roles in the growth inhibition triggered by UV-B exposure (Gómez et al., 2022). In addition, E2FB, together with E2FC and RBR1, has been found to be a part of DREAM (DP (dimerization partner), Rb (Retinoblastoma)-like, E2F, and MuvB) complexes, which are crucial for timely succession of transcriptional waves involved in cell cycle progression and/or onset of cell differentiation (Magyar et al., 2016; Lang et al., 2021). By contrast, E2FA is not copurified with DREAM complex subunits from plant cell extracts, although it can interact with some components in the yeast two-hybrid system, suggesting that it differs from E2FB in the strength of its association with DREAM complexes (Lang et al., 2021).

In addition to their role as cell cycle regulators, several lines of evidence indicate that E2Fs control the cellular response to DNA damage and replication stress. In mammals, *E2F1* transcription is usually inactivated at the start of S phase by induction of the repressive E2F6 protein, which is an E2F1 target (Giangrande et al., 2004). However, under DNA-damaging conditions, the E2F1 protein is stabilized by ATM- or ATR-dependent phosphorylation (Lin et al., 2001) and accumulates at the sites of DSBs (Biswas and Johnson, 2012). Additionally, during replication stress, the E2F6 repressor is inactivated, causing sustained *E2F1* transcription, which is necessary for arrest and stabilization of replication forks, and, in this way, prevents DNA damage (Bertoli et al., 2013, 2016). Remarkably, in cells with impaired checkpoint control, sustained transcription of *E2F1* is sufficient to alleviate DNA damage levels (Bertoli et al., 2016). Likewise, in tobacco BY-2 cells, the *NtE2F* gene is induced in response to high doses of UV-C (Lincker et al., 2004), and its protein localizes in distinct chromatin foci upon DNA damage (Lang et al., 2012), hinting at possible conservation of the role of E2F transcription factors in the DDR in plants. More recently, it has been found that, upon DNA damage, RBR1 also colocalizes with γH2AX, a histone variant that is phosphorylated by ATM and ATR and forms foci delineating breaks in the DNA (Friesner et al., 2005), and that this is necessary for correct localization of RAD51 foci (Biedermann et al., 2017). Using chemical inhibitors of ATM and ATR, it has also been found that formation of foci of E2FA and RBR1 is dependent on both kinases (Horvath et al., 2017), recruiting the DNA repair protein BRCA1 to these foci. Furthermore, E2FB has been shown to be required for cell cycle arrest induced by the cross-linking agent cisplatin (Lang et al., 2021). Collectively, these results provide strong evidence of a role of E2FA and E2FB in the cellular response to DSBs, although their contribution to the replication stress response has never been explored.

In this study, we studied the involvement of E2FA and E2FB in response to replication stress. Surprisingly, we show that E2FA and E2FB share numerous targets with SOG1. Further, we show that E2FB rather than E2FA activity is required to allow cell cycle progression despite replication stress. In-depth analysis of the expression behavior of common SOG1 and E2F targets demonstrates that E2FA and E2FB play complementary and distinct roles in this pathway.

RESULTS

E2FA and E2FB share some targets with SOG1

E2FA, E2FB, and RBR1 have all been shown recently to play a role in the plant DSB response (Biedermann et al., 2017; Horvath et al., 2017; Lang et al., 2021). Exploiting our recent analysis of E2FA and E2FB targets (Gombos et al., 2022), we investigated whether E2FA/B shared common targets with SOG1. When comparing the target genes of E2FA (Supplemental Table 1A), E2FB (Supplemental Table 1B), and SOG1, as determined by tandem chromatin affinity purification (Verkest et al., 2014) or chromatin immunoprecipitation sequencing (ChIP-seq) experiments (Bourbousse et al., 2018; Gombos et al., 2022), we found that a greater number of SOG1 target genes were also targeted by at least one of the two E2F transcription factors than what would be expected by chance (Fisher's exact test; Figure 1A; Supplemental Table 1C). Among these, the *WEE1* gene could be found, encoding a cell-cycle-inhibitory kinase implicated in the replication stress response (De Schutter et al., 2007). Interestingly, residual activation of the *WEE1* promoter was observed in response to HU-induced replication stress in a *sog1* mutant and required the E2F-binding site found in its promoter, confirming potential involvement of E2FA/B in the replication stress response (Figure 1F). We next compared the position of experimentally identified E2FA- and E2FB-binding sites with those identified previously for SOG1 (Bourbousse et al., 2018). E2FA and E2FB bound the common target genes at positions close to the SOG1-binding site (Figure 1B–1E; Supplemental Table 1C), suggesting that E2FA/B and SOG1 bind in close proximity to each other on their target promoters. The observation that E2FA/B can activate *WEE1* in response to HU independent of SOG1 (Figure 1F) and the significant overlap between putative E2FA/B and SOG1 target genes (Figure 1A) prompted us to test whether E2FA/B play a role in the replication stress response.

Loss of *E2FB* strongly aggravates growth defects triggered by replication stress

To explore the roles of E2FA and E2FB in the replication stress response, we used the hypomorphic mutant for Polε, *pol2a-4* (hereafter referred to as *pol2a*), which shows constitutive replication stress (Pedroza-Garcia et al., 2017), and generated double- and triple-mutant combinations between *pol2a*, *sog1*, and *e2fa* or *e2fb* mutants. Two independent transfer DNA insertion lines have been described for *E2FA* and *E2FB* (Berckmans et al., 2011a, 2011b). In the case of *E2FA*, the *e2fa-1* allele appears to be a null mutant lacking E2FA protein accumulation, whereas *e2fa-2* accumulates significant levels of a truncated protein (Leviczky et al., 2019). In the case of *E2FB*, the protein cannot be detected in protein extracts of *e2fb-1* or *e2fb-2* mutants (Leviczky et al., 2019). In terms of protein function, viable *e2fa e2fb* double mutants have been obtained using the *e2fa-2* but not the *e2fa-1* allele (Heyman et al., 2011), suggesting that the truncated protein accumulating in *e2fa-2* mutants is at least partially functional. For our genetic analysis, we therefore used only the *e2fa-1* mutant allele, in which *E2FA* loss of function is likely full, and both *e2fb* alleles. Throughout the manuscript, we show results obtained for the *e2fb-1* allele, but the *e2fb-2* allele systematically gave the same results. Phenotypically, *e2fa-1* and *e2fb-1* single mutants did not show growth reduction compared with the wild type (WT; Columbia-0 [Col-0]), whereas *pol2a* mutants were significantly smaller (Figure 2A and 2B). Growth reduction was more severe in the *pol2a sog1* double mutant, consistent with the hypersensitivity of the *sog1* mutant to replication stress (Pedroza-Garcia et al., 2017). The *pol2a e2fa-1* mutant rosette size was identical to that of the *pol2a* parent, whereas the *e2fb-1 pol2a* mutant was slightly smaller. Strikingly, the *e2fb-1 pol2a sog1* triple mutant showed a more severe growth defect than *pol2a sog1*, a phenomenon not observed with the *e2fa-1* mutation (Figure 2A and 2B). We also analyzed the root length of the various mutants and observed that E2FB, but not E2FA, is required for root growth in plants suffering from constitutive replication stress (Figure 2C). These data show that E2FB contributes to plant response to replication stress, allowing growth maintenance despite replication defects.

E2FB positively regulates meristem size and cell cycle progression in response to replication stress

The severe growth reduction observed in *e2fb-1 pol2a sog1* triple mutants and, to a lesser extent, in *e2fb-1 pol2a* double mutants likely results from cell proliferation defects. To test this hypothesis, we first measured the root meristem size in all genotypes. As shown in Figure 3, replication stress triggered by Polε deficiency resulted in reduced meristem size. Whereas this defect was not significantly aggravated in the absence of SOG1, root meristem length was further reduced in *ef2b-1 pol2a* and *e2fb-1 pol2a sog1* mutants (Figure 3B). Again, this effect was not observed in *e2fa-1 pol2a* and *e2fa-1 pol2a sog1* mutants (Figure 3B). These results confirmed that E2FB, but not E2FA, plays a crucial role in proliferating cells to protect them from cell proliferation arrest triggered by replication stress.

To further dissect how E2FB affects cell proliferation in response to replication stress, we decided to analyze cell cycle progression into more detail in all mutant combinations. We first analyzed cell cycle progression in root meristems using cumulative ethynyl-2′-deoxyuridine (EdU) incorporation (Hayashi et al., 2013), but EdU-positive cells represented a very large proportion of cells in the meristem of the *e2fb-1 pol2a sog1* triple mutant, and this proportion increased very slowly, making S phase and cell cycle length calculation extremely difficult (Supplemental Figure 1). As a proxy for S phase length, we therefore assessed the proportion of S phase cells using short EdU labelling (30 min). Delayed S phase progression causes S phase to account for a larger proportion of total cell cycle length and, thus, results in an increase in the proportion of S phase cells in the cell population. The proportion of nuclei in S phase was the same in the WT, single *sog1*,*e2fa-1* and *e2fb-1* mutants, and double *e2fa-1 sog1* and *e2fb-1 sog1* mutants (Figure 3C), while it increased in all mutant combinations holding the *pol2a* mutation, consistent with our previous findings (Pedroza-Garcia et al., 2017). Interestingly, it further increased in *pol2a sog1* and *e2fb1 pol2a* mutants and even more so in the *e2fb-1 pol2a sog1* triple mutant. By contrast, the *e2fa1* mutation had no impact on the proportion of S phase cells in any mutant combination. Next, to monitor G2-to-M progression, we performed pulse EdU labeling (30 min), followed by a 5-h thymidine chase (Figure 3D). Progression from G2 to M was

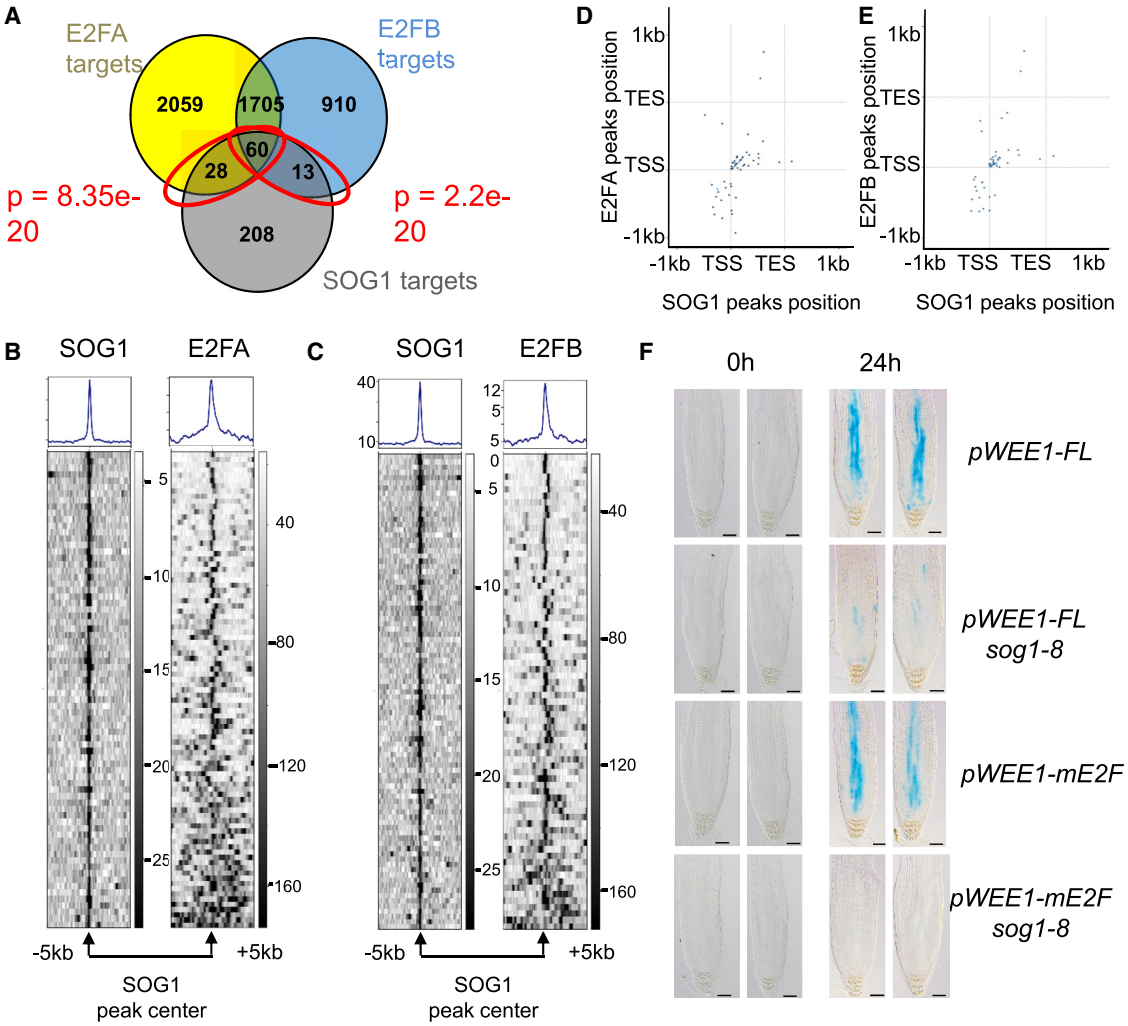

Figure 1. E2FA, E2FB, and SOG1 share common target genes and independently activate *WEE1*.

(A) Venn diagram showing the overlap between SOG1 (Bourbousse et al., 2018), E2FA (as defined by the union of targets found by tandem chromatin affinity purification [Verkest et al., 2014] and ChIP-seq [Gombos et al., 2022]; FDR < 0.05 and enrichment > 2.4), and E2Fb target genes (Gombos et al., 2022; FDR < 0.05, enrichment >2). Significance of overlap was estimated with Fisher's exact test (total number of loci: 38 194 according to Araport11; Cheng et al., 2017).

(B) Heatmaps showing E2FA and SOG1 binding on their common target genes, centered around the SOG1 binding site. SOG1 and E2FA binding sites are at very similar positions on most of their common targets, as illustrated by the metaplot above the heatmap.

(C) Heatmaps showing E2FB and SOG1 binding on their common target genes, centered around the SOG1 binding site. SOG1 and E2FB binding sites are at very similar positions on most of their common targets, as illustrated by the metaplot above the heatmap.

(D and E) Density plots showing overlap of SOG1 and E2FA **(D)** or E2FB **(E)** using a hexagonal binning routine on their common target genes. Each dot represents the distance from the peak midpoint to the nearest gene. The y axis shows the location of the E2FA **(D)** or E2FB **(E)** peak midpoint compared with gene position, while the x axis indicates the position of the SOG1 peak midpoint relative to the nearest gene. Most dots occur close to the diagonal of the graph, showing that E2FA/B and SOG1 bind neighboring sequences. TSS, transcription start site; TES, transcription end site.

(F) Constructs encompassing the full-length *WEE1* promoter driving expression of the beta-glucuronidase (*GUS*) gene were introduced into WT or *sog1-8* mutants. GUS staining was observed after 24 h of treatment with the replication stress-inducing drug HU (1 mM). Staining was drastically reduced but still visible in the *sog1-8* background. When the E2F binding site was deleted (*mE2F*), residual activation was lost, demonstrating that E2Fs can contribute to *WEE1* activation in response to replication stress. Scale bars, 50 μm.

delayed in *e2fb-1 pol2a* and even more so in *e2fb-1 pol2a sog1* mutants compared with *pol2a* and *pol2a sog1* mutants, respectively (Figure 3D). This phenomenon was not observed in *e2fa-1* mutant combinations. The same result was obtained using flow cytometry on flower buds, as indicated by a significant increase in the population of G2 nuclei at the expense of the number of G1 cells in the *e2fb-1 pol2a* and *e2fb-1 pol2a sog1* mutants compared with the WT, which was not observed in *pol2a* and *pol2a sog1* (Supplemental Figure 2). These data indicate that the same cell cycle defects are observed in different types of proliferating tissues.

Together, these data suggest that E2FB positively regulates cell cycle progression through G2 and onset of the G2/M transition in cells exposed to replication stress. This function seems to be particularly important in the absence of SOG1, suggesting that

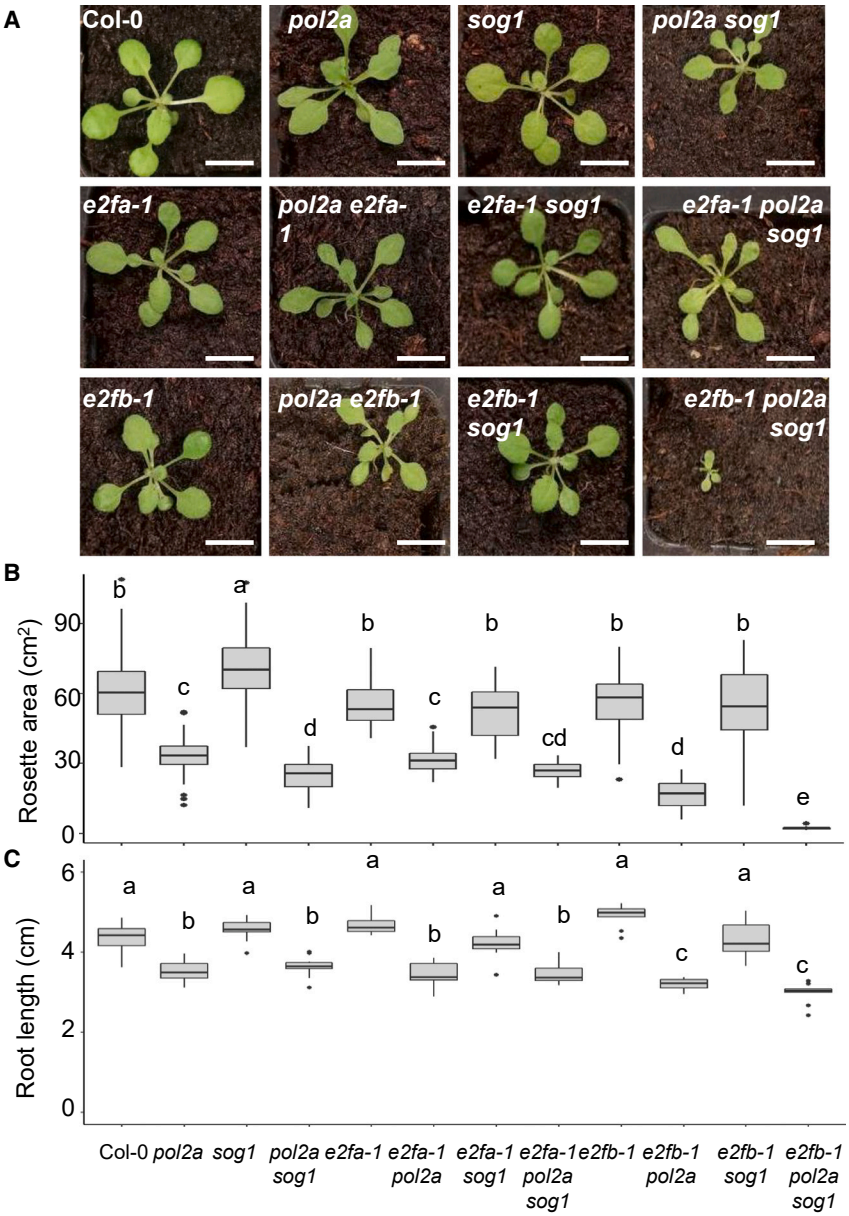

Figure 2. E2FB, but not E2FA, is required for sustained plant growth in response to replication stress.

(A) Representative rosette phenotype of 30-day-old plants of the indicated genotype. Scale bars, 1 cm. **(B and C)** Quantification of rosette area **(B)** and root length **(C)** in the indicated genotypes. Data are mean ± SD from at least 15 **(B)** or 10 **(C)** measurements for each line and are representative of two independent experiments. In boxplots, the vertical size of the boxes shows the interquartile range (IQR), and the whiskers correspond to 1.5× the IQR. The horizontal line corresponds to the median. Individual dots indicate values falling outside of this range. Significant differences from the WT are determined by one-way ANOVA with post hoc Tukey HSD (honestly significant difference). Different letters indicate statistically significant differences (ANOVA and Tukey test, $p < 0.05$ for B and $p < 0.01$ for C).

SOG1 and E2FB may act in parallel to maintain the proliferative capacity in cells exposed to replication stress .

Replication stress-induced genes are under dual control of E2Fs and SOG1

To gain insight into the mechanisms underlying the role of E2FB in the replication stress response, we compared gene expression changes in shoot apices of *pol2a*, *pol2a sog1*, and *e2fb-1 pol2a sog1* mutants (Supplemental Table 2). Compared with WT plants, we found 1822, 2599 and 3512 upregulated genes in *pol2a*, *pol2a sog1*, and *e2fb-1 pol2a sog1* mutants, respectively (false discovery rate [FDR] < 0.05). Among those, 1095 were commonly upregulated in all three mutant lines (Figure 4A; Supplemental Table 3). Gene Ontology (GO) analysis of these 1095 genes revealed a significant enrichment in GO terms such as DNA repair, DNA replication, and negative regulation of the cell cycle (Figure 4B), consistent with the constitutive replication stress triggered by *POL2A* deficiency and induced cell cycle defects (Pedroza-Garcia et al., 2017). Genes specifically upregulated in the *e2fb-1 pol2a sog1* mutant were not enriched in E2F target genes, indicating that most of them are likely regulated indirectly by E2Fs. Because DDR- and cell-cycle-related genes were enriched only in upregulated genes, we focused on these genes for further analyses.

To understand the behavior of SOG1 target genes in the different genotypes, we analyzed in more detail their expression level in *pol2a*, *pol2a sog1*, and *e2fb-1 pol2a sog1* mutants. Of the 309 SOG1 targets (Bourbousse et al., 2018), 78 were significantly upregulated (FDR < 0.05, $\log_2$FC > 0.5) in at least one genotype compared with the WT and were kept in the analysis. For each gene, we calculated a *Z* score based on its expression level in the different samples. This approach allowed us to define three main groups of genes with contrasted expression profiles (Figure 4C; Supplemental Table 4). The first group (comprising 19 genes) corresponded to genes mainly regulated by SOG1; they were induced in *pol2a*, but their expression returned to basal levels in *pol2a sog1* and *e2fb-1 pol2a sog1* mutants. Genes in group 2 were highly induced in *pol2a* mutants and had lower expression in *pol2a sog1* mutants, but their expression was increased in the triple mutant compared with *pol2a sog1*, indicating that they are antagonistically regulated by SOG1 and E2FB (30 genes; Figure 4C; Supplemental Table 4). Interestingly, group 2 genes were particularly enriched in E2F targets (about 60% of genes were identified as targets of at least one E2F; Supplemental Table 4), further supporting the hypothesis that they are under dual control of SOG1 and E2FB. Importantly, we could confirm by qRT-PCR on a subset of these genes that their expression was not affected by the *e2fa-1* mutation, supporting the hypothesis that they are

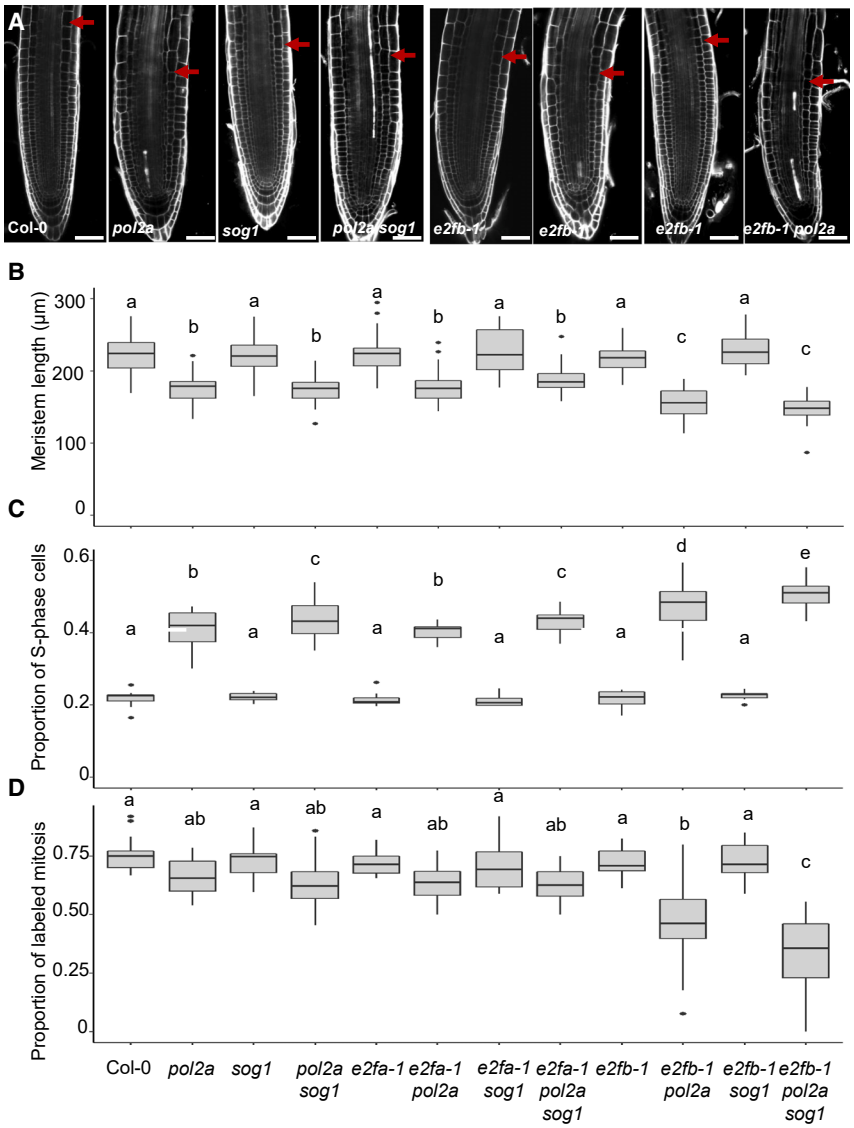

Figure 3. Loss of *E2FB*, but not *E2FA*, further reduces root apical meristem length in the *pol2a* background by delaying cell cycle progression.

(A) Representative confocal images of 7-day-old root apical meristems of WT (Col-0), *pol2a*, *sog1*, *pol2a sog1*, *e2fb-1*, *e2fb-1 pol2a*, *e2fb-1 sog1*, and *e2fb-1 pol2a sog1*. Cell walls were stained with propidium iodide (PI). Only mutant combinations with the *e2fb-1* mutation are shown because the *e2fa-1* mutation did not have any effect on the phenotype of *pol2a* or *pol2a sog1* mutants, as shown in **(B)**. Red arrows indicate the upper limit of the apical root meristem. Scale bars, 50 μm.

(B) Quantification of root meristem length in the indicated genotypes (n > 10). In boxplots, the vertical size of the boxes shows the IQR, and the whiskers correspond to 1.5× the IQR. The horizontal line corresponds to the median. Individual dots indicate values falling outside of this range. Different letters indicate statistically relevant differences (ANOVA followed by Tukey test, $p < 0.05$). Data are representative of three independent experiments.

(C) Pulse EdU labeling (30 min) was used to estimate the proportion of S phase cells in the meristems of the indicated genotypes. Measurements were done on at least 10 root tips (>500 nuclei per root tip).

(D) Mitosis in 5-day-old roots of all mutant lines labeled with ethynyl-2′-deoxyuridine (EdU). The boxplot represents the proportion of labeled mitosis in the indicated genotypes after 30 min of labeling followed by a 5-h thymidine chase. Data represent at least 15 roots and are representative of three independent experiments.

The vertical size of the boxes shows the IQR, and the whiskers correspond to 1.5x the IQR. The horizontal line corresponds to the median. Individual dots indicate values falling outside of this range. Different letters indicate statistically significant differences (binomial ANOVA followed by Tukey post hoc test, $p < 0.01$).

specifically repressed by E2FB (Supplemental Figure 3). Among these shared E2FB/SOG targets that appeared to be antagonistically controlled by SOG1 and E2FB, we found the *ANAC044* and *ANAC085* transcription factor genes that have been shown to negatively regulate G2/M progression. This result was confirmed by qRT-PCR (Supplemental Figure 4A). Interestingly, *ANAC044* and *ANAC085* are not only direct SOG1 and E2FB targets but also RBR1 targets (Gombos et al., 2022; Supplemental Figure 4B and 4C), suggesting that E2FB could repress them through its interaction with RBR1. Because these two transcription factors are involved in inhibition of the G2/M transition, their upregulation in *e2fb-1 pol2a sog1* mutants could account for the observed delay in G2 progression we observed in these mutants.

Finally, the transcriptomics results indicate that E2FA and E2FB could function redundantly to activate DDR genes independent of SOG1. Indeed, genes in group 3 (18 genes) were partially dependent on SOG1 for their induction, but their expression level remained high in triple mutants (Figure 4C), indicating that they are activated independent of SOG1 and E2FB. In addition, the majority (about 60%) of group 3 genes were identified as E2F targets, suggesting that E2FA could account for their activation in the absence of SOG1 and E2FB. Reciprocally, SOG1 targets were significantly enriched among genes upregulated in the *e2fb-1 pol2a sog1* triple mutant compared with the *pol2a sog1* mutant ($p = 1.118e{-}5$, Fisher's exact test, total number of genes detected in the RNA sequencing (RNA-seq) analysis = 20 946; Figure 4D), further confirming that *bona fide* SOG1 targets can be activated independent of SOG1 in response to replication stress. Interestingly, GO analysis of all genes that were specifically upregulated in *pol2a sog1* and *e2fb-1pol2a sog1* mutants and not in *pol2a* single mutants compared with WT plants revealed a significant enrichment in terms of relation to cell cycle regulation (Supplemental Figure 5A), and E2FA and E2FB targets were significantly enriched in this list (Supplemental Figure 5B). It is worth noting that E2F targets were also highly enriched among genes that were commonly upregulated in all three mutant lines (428 of 1095, $p = 8.179e{-}36$, Fisher's exact test, total number of genes detected in the RNA-seq

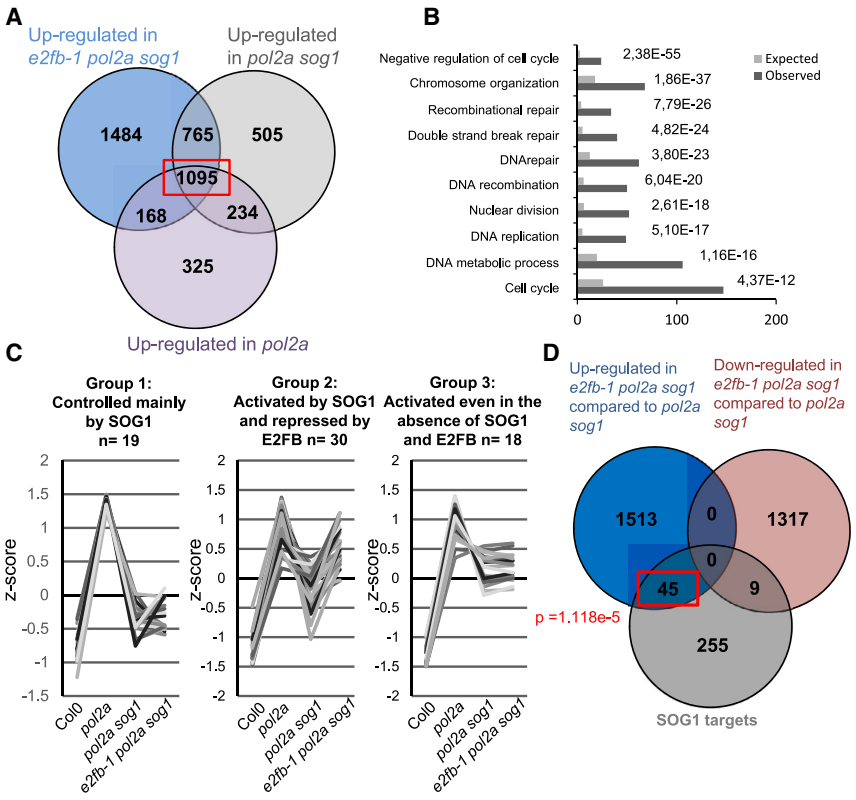

Figure 4. E2FB and SOG1 cooperate to control replication stress-induced transcriptional changes.

(A) Venn diagram showing the overlap between upregulated genes in *pol2a*, *pol2a sog1*, and *e2fb-1 pol2a sog1* compared with WT plantlets in the shoot apex. Apices were collected from 7-day-old plantlets by removing cotyledons and hypocotyls.

(B) GO term analysis of genes upregulated in all mutant lines.

(C) Graphs showing expression changes (using the *Z* scores available in Supplemental Table 4) of the three main categories of SOG1 targets that are misregulated in *pol2a*, *pol2a sog1*, and *e2fb-1 pol2a sog1* mutants.

(D) Overlap between SOG1 target genes and misregulated genes in triple mutants compared with *pol2a sog1* double mutants. SOG1 targets are significantly more represented amongst upregulated genes, indicating that E2FB acts as a repressor of these genes.

analysis = 20 946). These observations suggest that, although the *e2fa-1* mutation alone or in combination with *sog1* does not appear to affect the developmental defects caused by replication stress, E2FA could activate DDR genes but likely functions redundantly with E2FB to fulfill this role.

Together, these results indicate intricate regulation of DDR genes by SOG1 and E2Fs in response to replication stress. On one hand, E2FB plays an important role in mitigating DDR gene activation to allow sustained growth in response to replication stress, and on the other hand, E2FA and E2FB likely function redundantly to activate a subset of DDR genes synergistically and in parallel with SOG1.

E2FA, E2FB, and SOG1 cooperate to allow cell cycle progression in response to replication stress

To test the possibility that E2FA could contribute to the replication stress response in the absence of E2FB and SOG1, we used the partial loss-of-function allele of E2FA (*e2fa-2*) and generated *e2fa-2 e2fb-1 sog1* triple mutants. To induce replication stress, plantlets were exposed to the replication inhibitor HU. As published before, *sog1* mutants are slightly sensitive to replication stress (Hu et al., 2015), whereas *e2fa*, *e2fb*, and *e2fa-2 e2fb-1* showed no such hypersensitivity (Figure 5). The *e2fa* and *e2fb* mutant alleles behaved in the same way. Similarly, as observed in response to constitutive replication stress induced by the *pol2a* mutant (Figure 2B), *e2fb-1 sog1* but not *e2fa-1 sog1* double mutants were more sensitive to HU than *sog1* mutants, consistent with the hypothesis that E2FB plays a more prominent role than E2FA in the replication stress response. Strikingly, the *e2fa-2 e2fb-1 sog1* triple mutant displayed even stronger HU hypersensitivity, with root growth almost completely blocked after transfer to HU (Figure 5 and Supplemental Figure 6), and cell death induced in the root meristem, as indicated by cellular uptake of propidium iodide (PI) (Supplemental Figure 7). It is worth noting that using HU induces milder developmental defects than the *pol2a* mutation, possibly because it affects mainly roots that are directly in contact with the medium and because plants are kept on the drug for a short period of time. Nevertheless, these data clearly indicate a contribution of E2FA to the replication stress response when both E2FB and SOG1 are inactivated.

Because hindrance of fork progression is inevitable during S phase, we investigated whether E2F deficiency may trigger replication stress even in a WT background. Whereas Gómez et al. (2022) reported an increase in meristem size and cortical meristem cell number for the *e2fa-2 e2fb-1* mutant, under our own growth conditions we noticed no effect on meristem size but a statistically significant reduction in cell number (Supplemental Figure 8A–8C), indicative of activation of cell cycle arrest. Although the inhibition of cell proliferation could be due to the role of E2Fs as activators of cell cycle progression, it may also reflect an inefficient response to basal levels of replication stress that generally happen during S phase. In line with this hypothesis, we found that *e2fa-2 e2fb-1* double mutants displayed a prolonged S phase and increased total cell cycle length (Figure 6), whereas S and G2 phase duration was unaffected in *e2fa-2* or *e2fb-1* single mutants (Supplemental Figure 8D and 8E). Importantly, these defects were abolished in the *sog1* mutant background, indicating that E2F deficiency triggers replication stress, leading to SOG1-dependent cell cycle delay. To confirm this hypothesis, we performed an RNA-seq analysis on root tips of 7-day-old seedlings grown under control conditions. A total of 148 genes were found to be downregulated in the *e2fa-2 e2fb-1* mutant (FDR < 0.01), of which 73 are likely direct E2FA or E2FB target genes based on ChIP data (Figure 6C; Supplemental Table 5A and S5B). This list includes

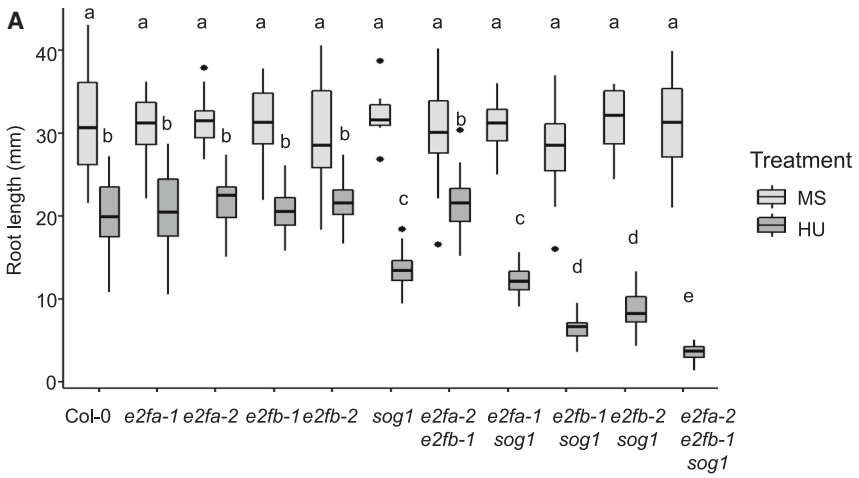

Figure 5. Simultaneous loss of *E2FA*, *E2FB*, and *SOG1* abolishes plant tolerance to replication stress.

(A) Plantlets were germinated on 0.5× MS medium and transferred to medium supplemented with 1 mM HU after 4 days. Root lengths were measured after 10 days. Data presented are mean ± SD (n > 20). Significant differences from the WT were determined by one-way ANOVA with post-hoc Tukey HSD. Different letters indicate statistically significant differences (ANOVA and Tukey test, $p < 0.01$). Representative images of plants are shown in Supplemental Figure 6.

described components of the DNA replication machinery (Supplemental Table 6) and GO enriched categories (obtained through http://geneontology.org/), including DNA replication initiation, DNA duplex unwinding, and chromatin assembly (Supplemental Table 7). Next to the 148 downregulated genes, we found 345 genes to be upregulated (FDR < 0.01, fold change [FC] > 1.5). Strikingly, according to the ChIP data, 145 of these are E2FA- or E2FB-bound genes (Figure 6C; Supplemental Table 5C), consistent with recent evidence showing that the canonical E2FA/B play a key role in repression of cell cycle genes, likely through their association with RBR1 (Gombos et al., 2022). GO categories enriched in the list of E2F-bound upregulated genes mainly indicate DNA repair, recombinational repair, and response to gamma irradiation and X-rays (Supplemental Table 8). qRT-PCR of a selected number of genes from down- and upregulated genes confirmed the RNA-seq results (Figure 6D and 6E). Strikingly, upregulated *PARP1* and *SMR7* gene expression in the *e2fa-2 e2fb-1* double mutant was repressed in the *e2fa-2 e2fb-1 sog1* triple mutant. Different from the *MCM9* gene that showed no transcriptional repression, the former two are *bona fide* SOG1 target genes, indicating that absence of E2FA and E2FB triggers a SOG1-dependent transcriptional response (Figure 6E). Accordingly, among the 345 genes upregulated in *e2fa-2 e2fb-1* double mutants, 43 were SOG1 targets (a number significantly greater than could be expected by chance; p = 7.746e−24, Fisher's exact test, total number of genes detected in the RNA-seq experiment = 17 028), further confirming that loss of E2FA and E2FB triggers replication stress and SOG1-dependent activation of DDR genes.

DISCUSSION

E2Fs are core cell cycle regulators that are evolutionarily conserved over most multicellular eukaryotes, including animals and the green lineage (Bertoli et al., 2013). Although functional diversification of E2Fs has been described in detail in animals (Ishida et al., 2001), our understanding of the specific functions of plant E2Fs remains limited.

E2FB plays a more prominent role than E2FA to allow plant growth in response to replication stress

Based on our observation that the *Arabidopsis* E2FA and E2FB transcription factors share several target genes with the central DDR regulator SOG1, we investigated their contribution to the plant replication stress response. We found that loss of E2FB, but not of E2FA, severely aggravated the developmental defects of the *pol2a-4* mutant, which suffers from constitutive replication stress (Pedroza-Garcia et al., 2017), as well as the sensitivity of the *sog1* mutant to the DNA replication-blocking drug HU. This requirement of E2FB for replication stress tolerance was particularly obvious in the *sog1* background, suggesting that E2FB and SOG1 act in parallel to cope with replication defects (Figure 7A). At the cellular level, we observed that progression from S to M phase was slower in these lines, suggesting that the length of G2 phase was increased by E2FB loss of function. Together, our results suggest that E2FB could allow progression of cells through G2/M phase under replication stress conditions.

We found that negative regulators of the cell cycle, such as *ANAC044* and *ANAC085*, are upregulated in *e2fb-1 pol2a sog1* mutants compared with *pol2a sog1* mutants, suggesting that E2FB may allow G2-to-M progression by inhibiting the repressors of the G2/M transition. Importantly, a role in allowing sustained cell proliferation in response to replication stress seems to be specific to E2FB because loss of E2FA did neither alter the sensitivity of *sog1* mutants to HU nor affect plant growth, meristem size, or the proportion of G2 cells in the *pol2a* or *pol2a sog1* mutants. These non-overlapping roles could relate to the fact that E2FB is more tightly associated with DREAM complexes than E2FA (Magyar et al., 2016; Lang et al., 2021). The function of these complexes is to bring together transcription factors that control G1/S genes (E2Fs) with the transcription factors controlling G2/M genes (MYB3Rs), which is essential for timely succession of transcriptional waves during the cell cycle and entry into quiescence during differentiation (Magyar et al., 2016). DREAM complexes could thus be required to maintain the proliferation capacity of cells during replication stress by repressing the expression of cell-cycle-inhibitory factors such as *ANAC044* and *ANAC085* (Supplemental Figure 4) or *SMR5* (Supplemental Table 4).

Nevertheless, *e2fa-2 e2fb-1 sog1* triple mutants were completely unable to grow in the presence of replication stress, indicating that E2FA also contributes to this cellular response. We propose that E2FA and E2FB could function redundantly to activate part of the DDR response. This hypothesis would explain the fact that a large set of DDR and cell-cycle-related genes remain highly

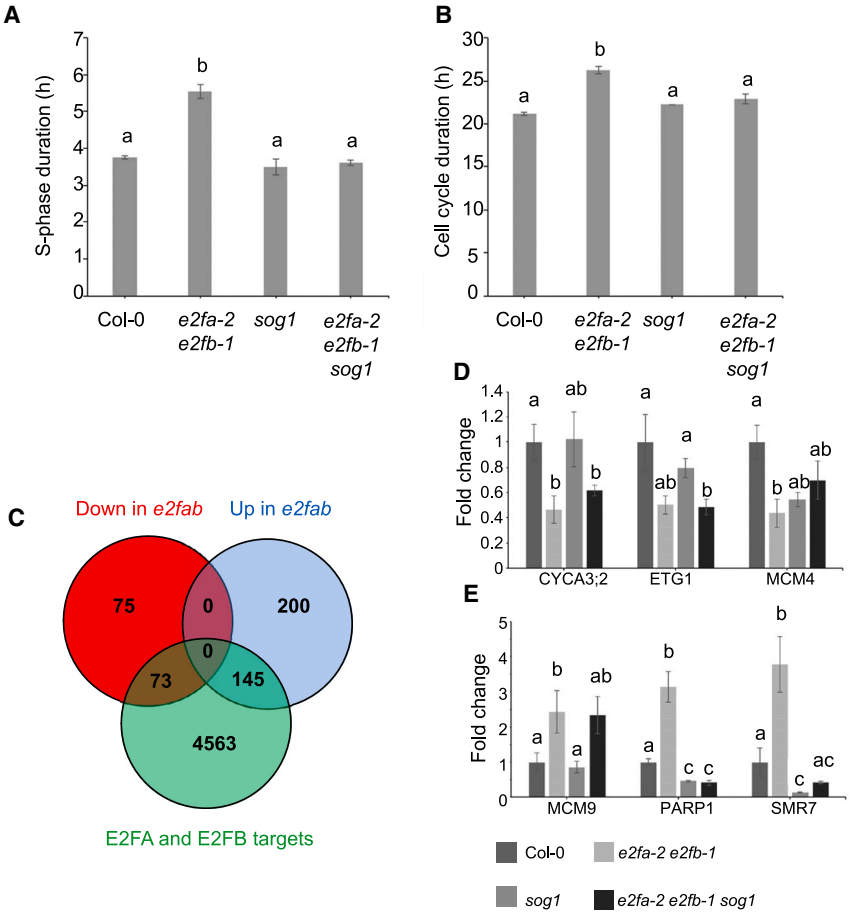

Figure 6. *E2F* deficiency triggers replication stress, SOG1-dependent cell cycle delay, and activation of DDR genes.

(A and B) S phase **(A)** and total cell cycle duration **(B)** were measured using a time course of EdU staining according to the protocol of Hayashi et al. (2013).

(C) Overlap between up- and downregulated genes in the *e2fa-2 e2fb-1* mutant against an experimental dataset of E2FA-bound genes (Verkest et al., 2014; Gombos et al., 2022).

(D and E) Relative expression levels of genes downregulated **(B)** or upregulated **(C)** in root tips of 7-day-old WT, *e2fa-2 e2fb-1 sog1*, and *e2fa-2 e2fb-1 sog1* mutant seedlings. Data represent mean ± SEM. The experiment was done in 3 technical and 3 biological repeats of at least 100 root tips. Significance was tested with Student's *t*-test. Means with different letters are significantly different ($p < 0.05$).

expressed in *e2fb-1 pol2a sog1* triple mutants. Importantly, the *e2fa-2* allele has been described as missing the transactivation and RBR1-interaction domain but retaining the "marked box" domain, which, in mammals, can provide a secondary interaction interface with RBR1 (Horvath et al., 2017) and still represses expression of DDR genes such as *BRCA1*, in contrast to the *e2fa-1* allele, which misses this interaction domain. We therefore cannot rule out the possibility that the dramatic phenotype of the *e2fa-2 e2fb-1 sog1* mutant could be due to inhibition of E2F target genes through binding of the residual E2FA in a complex with RBR1.

Complex transcriptional networks underlie the roles of E2FA/B and SOG1 in the replication stress response

A remarkable finding in this study is that activating E2FA/B and SOG1 induces a large set of common targets. Dual control of DDR genes by activating E2FA/B and SOG1 may allow fine-tuning of the gene expression level according to replication stress intensity. E2FA/B activity might account for basal induction levels during S phase, when cells are expected to be most sensitive to replication inhibitory stresses, whereas SOG1 might account for further activation in response to fork stalling. Likewise, in the *e2fa-2 e2fb-1* double mutant, we did not only see many E2F target genes being transcriptionally repressed but an even higher number of target genes to be induced, consistent with the notion that E2FA and E2FB largely function as corepressors by recruiting RBR1 to their targets (Gombos et al., 2022). Forty-three of these genes are SOG1 target genes, including *BRCA1* and *RAD51*. We hypothesize that these E2F target genes are essential for S phase progression as well as for repair of stalled replication forks and that, in *e2fa-2 e2fb-1* plants, SOG1 is activated because of replication defects. Such dual control of target genes by E2FA/B and SOG1 might explain the additive effects of the *e2fb-1* and *sog1* mutations seen on growth and cell cycle progression in the *pol2a* mutant as well as the increased sensitivity of the *e2fb-1 sog1* and *e2fb-2 sog1* double mutant and *e2fa-2 e2fb-1 sog1* triple mutant to HU. It probably also accounts for the almost complete stalling of cell cycle progression of the *e2fa-2 e2fb-1 sog1* triple mutant in the presence of HU. Another hypothesis that could explain the hypersensitivity of the *e2fa-2 e2fb-1 sog1* triple mutant to HU is the role of E2FA in DSB repair (Biedermann et al., 2017; Horvath et al., 2017). Defects in the replication stress response triggered by SOG1 and E2FB deficiency could lead to failure of fork stabilization mechanisms and accumulation of DSBs, which would require E2FA activation for repair.

Thus, the transcriptional network activated under replication stress is likely to be quite complex. Indeed, although E2FB and SOG1 share target genes, they seem to have opposite effects on expression of a significant proportion of their common targets. According to our transcriptomics analysis, we can distinguish three classes of genes among SOG1-regulated DDR genes (Figure 7B). The first set of genes seems to depend almost exclusively on SOG1 for expression because their induction is lost in *pol2a sog1* end *e2fb-1 pol2a sog1* plants (Figure 7B, class A genes). Consistent with this, this group of genes (corresponding to cluster 1 in Figure 4) is not statistically enriched in E2FA/B targets. By contrast, class B genes appear to be antagonistically regulated by SOG1 and E2FB because their expression is lower in *pol2a sog1* mutants than in *e2fb-1 pol2a sog1* mutants. This is the case, for example, for

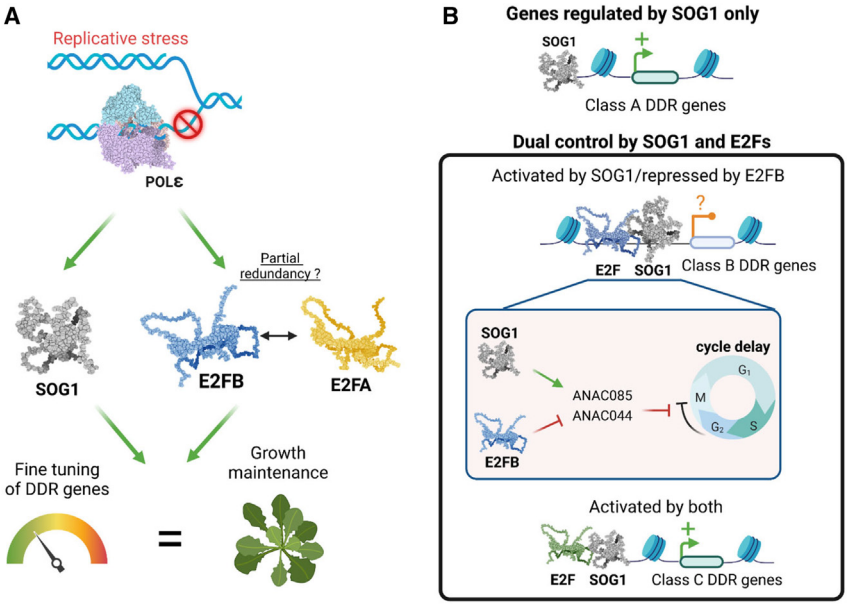

Figure 7. SOG1, E2FA, and E2FB act on distinct and common targets to fine-tune plant DDR.

(A) Our genetic analysis shows that SOG1 and E2Fs function independently to fine-tune DDR gene expression and allow sustained plant growth in response to replication stress.

(B) DDR genes can be distributed among three classes. One first set of genes (class A) depends only on SOG1 for activation. Class B genes are antagonistically regulated by SOG1 and E2FB, suggesting that E2FB could dampen SOG1-dependent cell cycle arrest to avoid complete developmental arrest. Among those, negative regulators of the cell cycle, such as ANAC085 and ANAC044, may contribute to the severe cell cycle arrest observed in *e2fb pol2a sog1* triple mutants. Class C genes are also targeted by SOG1 and E2FA/B and remain induced at similar levels by replication stress even in the absence of SOG1 and E2FB, suggesting that they are redundantly controlled by E2FA and E2FB. The image was created with BioRender.

ANAC044 and *ANAC085* (Figure 7B, inset). Together with the fact that these two genes have also been identified as direct RBR1 targets, this observation suggests that the repressor role of the E2FB–RBR1 complex, which we have described recently to be essential for maintenance of cell cycle quiescence (Gombos et al., 2022), also plays an important role in fine-tuning the plant DDR. Finally, a large set of DDR- and cell-cycle-related genes, among which is *WEE1*, were upregulated in the *pol2a* background, even in the absence of E2FB and SOG1 (class C genes), although SOG1 was required for full induction of their expression, suggesting involvement of a third partner, likely E2FA (Figure 7B). Importantly, this redundant role of E2FA and E2FB in regulation of DDR genes likely extends beyond SOG1 targets because we observed that a large number of cell cycle genes are E2F targets and remain highly expressed in the absence of SOG1 and E2FB, strongly suggesting that E2FA is also capable of activating them.

Our observations are reminiscent of the function of E2Fs during the replication stress response in mammalian cells. Indeed, in the absence of replication stress, a negative feedback loop between the repressor E2F6, which accumulates in late S phase, and activating E2Fs promotes the expression of E2F targets involved in DNA synthesis, such as proliferation cell nuclear antigen (Pennycook et al., 2020). In response to replication stress, the checkpoint kinase Chk1 phosphorylates and inhibits E2F6 (Bertoli et al., 2013), which allows activation of E2Fs to promote the expression of major replication, repair, and checkpoint effectors (Bertoli et al., 2016). This mechanism likely avoids an excessive delay in S phase progression and accumulation of DNA damage because of fork collapse. Although our observations point to a critical role of E2FB in control of the G2/M transition after replication stress, we cannot rule out that it could also be required to allow S phase progression despite replication stress. Such a hypothesis would match the observation that the increase in the proportion of EdU-labeled cells during cumulative EdU experiments was extremely slow in *e2fb-1 pol2a sog1* triple mutants. Thus, besides its likely role in control of the G2/M transition, E2FB could also function as a positive regulator of fork progression, and its loss of function might aggravate the replication defects of *pol2a* mutants.

Emerging roles of E2FA and E2FB in plant DDR

Together, our results point to a unique role of E2FB in the plant cell's response to replication stress. Interestingly, there is accumulating evidence showing that plant E2Fs are involved in maintenance of genome integrity and play essential roles in several aspects of the DDR and even DNA repair, consistent with the functions of their animal counterparts. Indeed, E2FA (Lang et al., 2021) and RBR1 form foci at DSBs and function independent of SOG1 to promote their repair, likely through their ability to interact with DNA repair proteins (Biedermann et al., 2017; Horvath et al., 2017). In addition, genome-wide identification of target genes revealed that RBR1 controls a large set of DDR genes (Bouyer et al., 2018), suggesting that E2F–RBR1 complexes may control expression of DDR genes and directly contribute to DNA repair. The respective roles of E2FA/B in the cellular response to DSBs are beginning to be unraveled, and both factors seem to contribute; E2FA by promoting DNA repair (Biedermann et al., 2017; Horvath et al., 2017) and E2FB possibly by triggering cell cycle arrest, although the two *e2fb-1* alleles do not affect this process in the same way (Lang et al., 2021). Conversely, our results suggest that E2FB is more prominently involved in the cellular response to replication stress in parallel with SOG1 and that E2FA plays only a minor role, possibly because E2FB can substitute for its activity. Only in the absence of E2FB did the *e2fa* mutation trigger sensitivity to replication stress, correlated with a longer S phase and cell cycle duration that depended on SOG1 activity. Recently, E2FA and E2FB have been shown to play distinct roles in the UV-B response (Gómez et al., 2022), as shown previously for E2FC (Gómez et al., 2019). It is therefore likely that plant E2Fs are involved in many aspects of the DDR to promote genome

integrity and avoid complete cell cycle arrest triggered by DNA stress. Our transcriptome analysis reveals the extreme complexity of the transcriptional networks involving E2Fs in response to replication stress. We have only scratched the surface of the process, but more refined studies will be required to understand the sequence of events occurring at the gene expression level and how the interplay between E2FA, E2FB, SOG1, and potentially other E2F family members allows exquisite regulation of cell cycle and DNA repair genes to maintain growth without compromising genomic integrity.

METHODS

Plant material and growth conditions

All *Arabidopsis thaliana* mutant lines used in this study are in the Col-0 background and have been described previously. The *e2fa-1* (*MPIZ_244*), *e2fa-2* (*GABI-348E09*), *e2fb-1* (*SALK_103138*), and *e2fb-2* (*SALK_120959*) mutants were first described in Berckmans et al. (2011a, 2011b). Except for analysis of *WEE1* promoter activity, the *sog1-1* mutant was isolated in the L*er* background (Yoshiyama et al., 2009) but later introgressed in the Col-0 background and was a kind gift from Anne Britt. The *sog1-101* allele has been described in Ogita et al. (2018). The *pol2a-4* mutant has been described in Yin et al. (2009) and further characterized in Pedroza-Garcia et al. (2017).

Seeds were sterilized using 5 ml Bayrochlore and 45 μl of absolute ethanol for 7 min, then washed three times with sterile water and kept at 4°C for 2 days. Seeds were sown on commercially available 0.5× Murashige and Skoog (MS; Duchefa) medium solidified with 0.8% agar (Phyto-Agar HP696, Kalys). Then, plates were transferred to long days (16 h light, 8 h dark, Lumilux Cool White lm, 50–70 μmol m^{-2} s^{-1}, 21°C) in an *in vitro* growth chamber. After 2 weeks, plantlets were transferred to soil, kept under short-day conditions (8 h light at 20°C, 16 h dark at 18°C) for a week, and then transferred to a long-day growth chamber (16 h light, 8 h dark, 21°C).

Generation of reporter lines

To construct the transcriptional reporter *pWEE1-GUS*, the full-length promoter region of the *WEE1* gene was PCR amplified (593 bp upstream of the translational start codon) and cloned into the pDONRP4-P1R entry vector by Gateway BP (base pairs) reaction. Site-directed mutagenesis was carried out to mutate the E2F-binding site GCGCGCAA at the −75 bp position to AACACTGT. Subsequently, the WT (*pWEE1-FL*) and mutated (*pWEE1-mE2F*) promoter were transferred into the pMK7S*NFm14GW,0 destination vector by Gateway LR reaction. Both constructs were transferred into the *Agrobacterium tumefaciens* C58C1RifR strain harboring the pMP90 plasmid. The obtained *Agrobacterium* strains were used to generate stably transformed *Arabidopsis* lines with the floral dip transformation method (Clough and Bent, 1998).

Root growth assay

Seeds were germinated on 0.5× MS medium, and after 4 days, seedlings were transferred to fresh plates of 0.5× MS medium or 0.5× MS medium supplemented with 1 mM HU. Plates were kept in a vertical position for about 2 weeks under long-day conditions. After 10 weeks, plates were scanned, and images were used to measured root length by Fiji software (https://imagej.net/Fiji).

Flow cytometry

Flow cytometry was done on flower buds of *e2f* combination mutants. Flowers buds were chopped with a razor blade. Then 1 ml of nucleus isolation buffer (45 mM $MgCl_2$, 30 mM sodium citrate, 60 mM MOPS, 1% (w/v) polyvinylpyrrolidone 10 000 [pH 7.2]) containing 0.1% (w/v) Triton X-100 and supplemented with 5 mM sodium metabisulphite and RNase (5 U/ml). The solution was filtered, and PI was added to the solution to a final concentration of 50 μg/ml. The DNA content of 5000–10 000 stained nuclei was determined using a Cyflow SL3 flow cytometer (Partec-Sysmex) with a 532-nm solid-state laser (30 mW) excitation and an emission collected after a 590-nm long-pass filter. For cell cycle analysis, we used the algorithm available in the FloMax software (flomax.software.informer.com).

EdU labeling

Seeds were germinated on 0.5× MS medium, and 5-day-old seedlings were transferred to 0.5× MS medium supplemented with 10 μM EdU for 30 min. We next performed a thymidine chase by transferring plantlets to 0.5× MS medium supplemented with an excess concentration of thymidine (100 μM). Plantlets were fixed after the 30-min EdU pulse or after a 4.5-h chase with 4% (w/v) paraformaldehyde dissolved in PME buffer (50 mM PIPES [pH 6.9], 5 mM $MgSO_4$, 1 mM EGTA) for 15 min under a vacuum. After that, plantlets were washed twice with PME to remove the traces of paraformaldehyde. Squares were drawn on polysine slides using a hydrophobic marker, and root tips were cut in a drop of PME under a stereomicroscope. The PME solution was then replaced by an enzyme solution (1% [w/v] cellulase, 0.5% [w/v] cytohelicase, 1% [w/v] pectolyase in PME), and samples were incubated for 1 h in a humid chamber at 37°C. Root tips were then washed three times with 1× PME. After removing most of the liquid, root tips were squashed under a coverslip. Slides were immersed in liquid nitrogen for about 15 s, and then the coverslip was carefully removed. Slides were dried overnight. The next day, slides were washed with 1× PBS (phosphate-buffer saline, Sigma) and then with 3% BSA (w/v) prepared in 1× PBS. Samples were permeabilized in 0.5% Triton dissolved in 1× PBS for 30 min. Slides were washed twice with 3% BSA + 1× PBS, and then the samples were incubated using the Click-iT Plus EdU Alexa Fluor 488 Imaging Kit (Thermo Fisher Scientific) according to the manufacturer's instructions for 30 min in the dark at room temperature. After washing once with PBS (pH 7.4) + BSA 3%, the nuclei were stained with Hoechst 33342 (1 μg/mL). Slides were mounted in Vectashield and observed using an epifluorescence microscope equipped with an Apotome module (AxioImager Z.2, Carl Zeiss) fitted with a metal halide lamp and the appropriate filter sets for imaging DAPI and Alexa 488 dyes. Images were acquired with a cooled CCD camera (AxioCam 506 monochrome, Carl Zeiss) operated using the Zen Blue software (Carl Zeiss).

Meristem length measurement

To measure the apical root meristem, 7-day-old root tips were stained with 10 μM PI for about 5 min and then observed with a Carl Zeiss LSM 880 laser-scanning confocal microscope using

a 561-nm laser for excitation. Fluorescence was acquired between 470 nm and 700 nm. Representative images were collected from 10–15 roots with 3 biological replicates. Meristem length was estimated by measuring the distance from the quiescent center to the first elongating cell in the cortex cell file.

Beta-glucuronidase (GUS) staining

For GUS staining, whole seedlings were stained in a 6-well plate (Falcon 3046, Becton Dickinson) as described previously (Beeckman and Engler, 1994). Briefly, plants were fixed in an ice-cold 80% (v/v) acetone solution for 30 min. Samples were washed three times with phosphate buffer (14 mM NaH_2PO_4 and 36 mM Na_2HPO_4) before being incubated in staining buffer (0.5 mg/ml 5-bromo-4-chloro-3-indolyl-b-D-glucuronic acid, 0.165 mg/ml potassium ferricyanide, 0.211 mg/ml potassium ferrocyanide, 0.585 mg/ml EDTA [pH 8], and 0.1% [v/v] Triton-X100, dissolved in phosphate buffer) at 37°C for 1 h. Samples mounted in lactic acid were observed and photographed with a stereomicroscope (Olympus BX51 microscope).

RNA extraction, RNA-seq library preparation, and qRT-PCR

For RNA-seq on shoot apices, total RNA was extracted from the shoot apex (first 2 leaves and meristematic zone) of 30 7-day-old plantlets using the RNA-Plus Kit (Macherey-Nagel), and libraries were prepared with 1 μg of total RNA using the NEBNext Ultra II RNA Library Prep Kit for Illumina according to the manufacturer's instructions. For RNA-seq experiments performed on root tips, the first 2 mm of 7-day-old seedlings were collected in liquid nitrogen. RNA from samples was extracted using the RNeasy Plant Mini Kit (QIAGEN), and cDNA was prepared from 1 μg of RNA using the iScript cDNA Synthesis Kit (Bio-Rad) according to the manufacturers' protocols. Libraries were sequenced on a HiSeq2000 or NextSeq500 75-bp single-end run.

qRT-PCR was performed in a final volume of 5 μl with SYBR Green I Master (Roche) and analyzed with a Lightcycler 480 (Roche) or LC96 (Roche). For each reaction, three biological and three technical repeats were performed. Primers used in this study are listed in Supplemental Table 9.

RNA-seq data analysis

Single-end sequencing of RNA-seq samples were trimmed using Trimmomatic-0.38 (Bolger et al., 2014) with the following parameters: minimum length of 30 bp, mean Phred quality score greater than 30, and leading and trailing base removal with base quality < 5. Bowtie2 Aligner (Langmead and Salzberg, 2012) was used for mapping to the TAIR11 genome assembly. Raw read counts were used to identify differentially expressed genes using the DiCoExpress package (Lambert et al., 2020).

ChIP-seq assay

ChIP-seq was done on 2-week-old plantlets expressing the E2FB-GFP fusion. Plantlets were cross-linked in 1% (v/v) formaldehyde for 15 min. Cross-linking was then quenched with 125 mM glycine for 5 min. Cross-linked plantlets were ground in liquid nitrogen, and nuclei were isolated in nucleus lysis buffer (0.1% SDS, 50 mm Tris-HCl [pH 8], 10 mM EDTA [pH 8]). Chromatin was sonicated for 7 min using Covaris S220 (peak power, 175; cycles/burst, 200; duty factor, 20). The sonicated chromatin was then immunoprecipitated using anti-GFP antibodies (Abcam, ab290) and incubated at 4°C overnight on a rotating wheel. Immunocomplexes were recovered with 40 μl of Dynabead protein A (Invitrogen, 10002D) and incubated for 2 h at 4°C with rotation. Immunoprecipitated material was washed 6 times for 5 min with ChIP dilution buffer (1.1% Triton X-100, 1.2 mM EDTA, 16.7 mM Tris-HCl [pH 8], 167 mM NaCl, protease inhibitors) and twice in TE (1 mm Tris-HCl [pH 8], 1 mM EDTA [pH 8]). ChIPed DNA was eluted by 2 15-min incubations at 65°C with 200 μl of freshly prepared elution buffer (1% SDS, 0.1 m $NaHCO_3$). Chromatin was reverse cross-linked by adding 16 μl of 5 M NaCl and incubated overnight at 65°C. The next day, chromatin was treated with RNase and Proteinase K and incubated for 3 h at 50°C, and DNA was extracted with phenol-chloroform. Ethanol was used to precipitate DNA in the presence of GlycoBlue, which was then resuspended in 10 μl of nuclease-free water. Libraries were then generated using 10 ng of DNA with the NEBNext Ultra II DNA Library Prep Kit for Illumina (New England Biolabs). The quality of the libraries was assessed with the Agilent 2100 Bioanalyzer, and the libraries were subjected to 1 × 7 bp high-throughput sequencing by NextSeq 500 (Illumina).

Statistical analysis

Statistical analyses were performed as indicated in the figure legends.

DATA AND CODE AVAILABILITY

RNA-seq raw data from this study were deposited into the Gene Expression Omnibus (GEO: GSE220849 for RNA-seq data obtained on root tips of *e2fa-2 e2fb-1* mutants and GEO: GSE220872 for transcriptome data obtained in *pol2a*, *e2fb-1 pol2a*, and *e2fb-1 pol2a sog1* mutants). Analysis of ChIP-seq raw data is described in more detail in Gombos et al. (2022), but raw data are available in the Gene Expression Omnibus (GEO: GSE218481). Sequence data from this article can be found in the *Arabidopsis* Genome Initiative or GenBank/EMBL databases under the following accession numbers: *E2FA* (At2g36010), *E2FB* (At5g22220), *POL2A* (AT1G08260), and *SOG1*(AT1g25580).

SUPPLEMENTAL INFORMATION

Supplemental information is available at *Molecular Plant Online*.

FUNDING

This work was supported by grants from the Research Foundation Flanders (G011420N) and Agence Nationale de la Recherche (21-CE20-0027).

AUTHOR CONTRIBUTIONS

L.D.V., M.B., and C.R. conceived and designed the research. M.N., C. Bergis, J.-A.P.-G., C.M., I.V., T.C., J.D.-W., R.B.-C., T.E., L.C., and D.L. performed the experiments. M.N., T.E., X.H., C. Bergis, C. Bergounioux, K.V., M.B., L.D.V., and C.R. analyzed data. L.D.V., M.B., and C.R. wrote the article. All authors read, revised, and approved the article.

ACKNOWLEDGMENTS

The authors thank Etienne Delannoy at Marie-Laure Martin-Magniette (IPS2) for advice regarding RNA-seq data analysis and Annick Bleys for critical reading and editing of the manuscript. Imaging experiments conducted at IPS2 benefitted from the imaging facility of the institute. No conflict of interest is declared.

Received: January 27, 2023
Revised: June 22, 2023
Accepted: July 3, 2023
Published: July 6, 2023

REFERENCES

Beeckman, T., and Engler, G. (1994). An easy technique for the clearing of histochemically stained plan tissue. Plant Mol. Biol. Rep. **12**:37–42.

Berckmans, B., Vassileva, V., Schmid, S.P., Maes, S., Parizot, B., Naramoto, S., Magyar, Z., Alvim Kamei, C.L., Koncz, C., Bogre, L., et al. (2011a). Auxin-dependent cell cycle reactivation through transcriptional regulation of Arabidopsis E2Fa by lateral organ boundary proteins. Plant Cell **23**:3671–3683.

Berckmans, B., Lammens, T., Van Den Daele, H., Magyar, Z., Bögre, L., De Veylder, L., Bogre, L., and De Veylder, L. (2011b). Light-dependent regulation of DEL1 is determined by the antagonistic action of E2Fb and E2Fc. Plant Physiol. **157**:1440–1451.

Bertoli, C., Klier, S., McGowan, C., Wittenberg, C., and De Bruin, R.A.M. (2013). Chk1 inhibits E2F6 repressor function in response to replication stress to maintain cell-cycle transcription. Curr. Biol. **23**:1629–1637.

Bertoli, C., Herlihy, A.E., Pennycook, B.R., Kriston-Vizi, J., and de Bruin, R.A.M. (2016). Sustained E2F-Dependent Transcription Is a Key Mechanism to Prevent Replication-Stress-Induced DNA Damage. Cell Rep. **15**:1412–1422.

Biedermann, S., Harashima, H., Chen, P., Heese, M., Bouyer, D., Sofroni, K., and Schnittger, A. (2017). The retinoblastoma homolog RBR1 mediates localization of the repair protein RAD51 to DNA lesions in *Arabidopsis*. EMBO J. **36**:1279–1297.

Biswas, A.K., and Johnson, D.G. (2012). Transcriptional and nontranscriptional functions of E2F1 in response to DNA damage. Cancer Res. **72**:13–17.

Bolger, A.M., Lohse, M., and Usadel, B. (2014). Trimmomatic: a flexible trimmer for Illumina sequence data. Bioinformatics **30**:2114–2120.

Bourbousse, C., Vegesna, N., and Law, J.A. (2018). SOG1 activator and MYB3R repressors regulate a complex DNA damage network in Arabidopsis. Proc. Natl. Acad. Sci. USA **115**:E12453–E12462.

Bouyer, D., Heese, M., Chen, P., Harashima, H., Roudier, F., Grüttner, C., and Schnittger, A. (2018). Genome-wide identification of RETINOBLASTOMA RELATED 1 binding sites in Arabidopsis reveals novel DNA damage regulators. PLoS Genet. **14**, e1007797.

Cheng, C.Y., Krishnakumar, V., Chan, A.P., Thibaud-Nissen, F., Schobel, S., and Town, C.D. (2017). Araport11: a complete reannotation of the *Arabidopsis thaliana* reference genome. Plant J **89**:789–804.

Clough, S.J., and Bent, A.F. (1998). Floral dip: a simplified method for Agrobacterium-mediated transformation of Arabidopsis thaliana. Plant J. **16**:735–743.

De Schutter, K., Joubès, J., Cools, T., Verkest, A., Corellou, F., Babiychuk, E., Van Der Schueren, E., Beeckman, T., Kushnir, S., Inzé, D., and De Veylder, L. (2007). Arabidopsis WEE1 kinase controls cell cycle arrest in response to activation of the DNA integrity checkpoint. Plant Cell **19**:211–225.

De Veylder, L., Beeckman, T., Beemster, G.T.S., de Almeida Engler, J., Ormenese, S., Maes, S., Naudts, M., Van Der Schueren, E., Jacqmard, A., Engler, G., and Inzé, D. (2002). Control of proliferation, endoreduplication and differentiation by the Arabidopsis E2Fa-DPa transcription factor. EMBO J. **21**:1360–1368.

del Pozo, J.C., Boniotti, M.B., and Gutierrez, C. (2002). Arabidopsis E2Fc functions in cell division and is degraded by the ubiquitin-SCF(AtSKP2) pathway in response to light. Plant Cell **14**:3057–3071.

Friesner, J.D., Liu, B., Culligan, K., and Britt, A.B. (2005). Ionizing radiation-dependent gamma-H2AX focus formation requires ataxia telangiectasia mutated and ataxia telangiectasia mutated and Rad3-related. Mol. Biol. Cell **16**:2566–2576.

Giangrande, P.H., Zhu, W., Schlisio, S., Sun, X., Mori, S., Gaubatz, S., and Nevins, J.R. (2004). A role for E2F6 in distinguishing G1/S- and G2/M-specific transcription. Genes Dev. **18**:2941–2951.

Gombos, M., Raynaud, C., Nomoto, Y., Molnár, E., Brik-Chaouche, R., Takatsuka, H., Zaki, A., Bernula, D., Latrasse, D., Mineta, K., et al. (2022). The canonical E2Fs together with RETINOBLASTOMA-RELATED are required to establish quiescence during plant development. bioRxiv **6**:2022. https://doi.org/10.1101/2022.12.05.519120.

Gómez, M.S., Ferreyra, M.L.F., Sheridan, M.L., Casati, P., Falcone Ferreyra, M.L., Sheridan, M.L., and Casati, P. (2019). Arabidopsis E2Fc is required for the DNA damage response under UV-B radiation epistatically over the microRNA396 and independently of E2Fe. Plant J. **97**:749–764.

Gómez, M.S., Sheridan, M.L., and Casati, P. (2022). E2Fb and E2Fa transcription factors independently regulate the DNA damage response after ultraviolet B exposure in Arabidopsis. Plant J. **109**:1098–1115.

Hayashi, K., Hasegawa, J., and Matsunaga, S. (2013). The boundary of the meristematic and elongation zones in roots: endoreduplication precedes rapid cell expansion. Sci. Rep. **3**:2723.

Heyman, J., Van den Daele, H., De Wit, K., Boudolf, V., Berckmans, B., Verkest, A., Alvim Kamei, C.L., De Jaeger, G., Koncz, C., and De Veylder, L. (2011). Arabidopsis ULTRAVIOLET-B-INSENSITIVE4 maintains cell division activity by temporal inhibition of the anaphase-promoting complex/cyclosome. Plant Cell **23**:4394–4410.

Horvath, B.M., Kourova, H., Nagy, S., Nemeth, E., Magyar, Z., Papdi, C., Ahmad, Z., Sanchez-Perez, G.F., Perilli, S., Blilou, I., et al. (2017). Arabidopsis RETINOBLASTOMA RELATED directly regulates DNA damage responses through functions beyond cell cycle control. EMBO J. **36**:1261–1278.

Hu, Z., Cools, T., Kalhorzadeh, P., Heyman, J., and De Veylder, L. (2015). Deficiency of the Arabidopsis helicase RTEL1 triggers a SOG1-dependent replication checkpoint in response to DNA cross-links. Plant Cell **27**:149–161.

Ishida, S., Huang, E., Zuzan, H., Spang, R., Leone, G., West, M., and Nevins, J.R. (2001). Role for E2F in control of both DNA replication and mitotic functions as revealed from DNA microarray analysis. Mol. Cell Biol. **21**:4684–4699.

Lambert, I., Paysant-Le Roux, C., Colella, S., and Martin-Magniette, M.-L. (2020). DiCoExpress: a tool to process multifactorial RNAseq experiments from quality controls to co-expression analysis through differential analysis based on contrasts inside GLM models. Plant Methods **16**:68.

Lammens, T., Li, J., Leone, G., and De Veylder, L. (2009). Atypical E2Fs: new players in the E2F transcription factor family. Trends Cell Biol. **19**:111–118.

Lang, J., Smetana, O., Sanchez-Calderon, L., Lincker, F., Genestier, J., Schmit, A.-C., Houlné, G., and Chabouté, M.E. (2012). Plant γH2AX foci are required for proper DNA DSB repair responses and colocalize with E2F factors. New Phytol. **194**:353–363.

Lang, L., Pettkó-Szandtner, A., Tunçay Elbaşı, H., Takatsuka, H., Nomoto, Y., Zaki, A., Dorokhov, S., De Jaeger, G., Eeckhout, D., Ito, M., et al. (2021). The DREAM complex represses growth in response to DNA damage in Arabidopsis. Life Sci. Alliance **4**, e202101141.

Langmead, B., and Salzberg, S.L. (2012). Fast gapped-read alignment with Bowtie 2. Nat Methods **9**:357–359.

Leviczky, T., Molnár, E., Papdi, C., Őszi, E., Horváth, G.V., Vizler, C., Nagy, V., Pauk, J., Bögre, L., and Magyar, Z. (2019). E2FA and E2FB transcription factors coordinate cell proliferation with seed maturation. Development **146**:dev179333.

Li, X., Cai, W., Liu, Y., Li, H., Fu, L., Liu, Z., Xu, L., Liu, H., Xu, T., and Xiong, Y. (2017). Differential TOR activation and cell proliferation in Arabidopsis root and shoot apexes. Proc. Natl. Acad. Sci. USA **114**:2765–2770.

Lin, W.C., Lin, F.T., and Nevins, J.R. (2001). Selective induction of E2F1 in response to DNA damage, mediated by ATM-dependent phosphorylation. Genes Dev. **15**:1833–1844.

Lincker, F., Philipps, G., and Chabouté, M.E. (2004). UV-C response of the ribonucleotide reductase large subunit involves both E2F-mediated gene transcriptional regulation and protein subcellular relocalization in tobacco cells. Nucleic Acids Res. **32**:1430–1438.

Magyar, Z., Bögre, L., and Ito, M. (2016). DREAMs make plant cells to cycle or to become quiescent. Curr. Opin. Plant Biol. **34**:100–106.

Maréchal, A., and Zou, L. (2013). DNA damage sensing by the ATM and ATR kinases. Cold Spring Harb. Perspect. Biol. **5**:a012716. https://doi.org/10.1101/cshperspect.a012716.

Mariconti, L., Pellegrini, B., Cantoni, R., Stevens, R., Bergounioux, C., Cella, R., and Albani, D. (2002). The E2F family of transcription factors from Arabidopsis thaliana. Novel and conserved components of the retinoblastoma/E2F pathway in plants. J. Biol. Chem. **277**:9911–9919.

Mazouzi, A., Velimezi, G., and Loizou, J.I. (2014). DNA replication stress: Causes, resolution and disease. Exp. Cell Res. **329**:85–93.

Müller, H., Bracken, A.P., Vernell, R., Moroni, M.C., Christians, F., Grassilli, E., Prosperini, E., Vigo, E., Oliner, J.D., and Helin, K. (2001). E2Fs regulate the expression of genes involved in differentiation, development, proliferation, and apoptosis. Genes Dev. **15**:267–285.

Naouar, N., Vandepoele, K., Lammens, T., Casneuf, T., Zeller, G., van Hummelen, P., Weigel, D., Rätsch, G., Inzé, D., Kuiper, M., et al. (2009). Quantitative RNA expression analysis with Affymetrix Tiling 1.0R arrays identifies new E2F target genes. Plant J. **57**:184–194.

Nisa, M.-U., Huang, Y., Benhamed, M., and Raynaud, C. (2019). The Plant DNA Damage Response: Signaling Pathways Leading to Growth Inhibition and Putative Role in Response to Stress Conditions. Front. Plant Sci. **10**:653.

Nisa, M., Bergis, C., Pedroza-Garcia, J.A., Drouin-Wahbi, J., Mazubert, C., Bergounioux, C., Benhamed, M., and Raynaud, C. (2021). The plant DNA polymerase theta is essential for the repair of replication-associated DNA damage. Plant J. **106**:1197–1207.

Ogita, N., Okushima, Y., Tokizawa, M., Yamamoto, Y.Y., Tanaka, M., Seki, M., Makita, Y., Matsui, M., Okamoto-Yoshiyama, K., Sakamoto, T., et al. (2018). Identifying the target genes of SUPPRESSOR OF GAMMA RESPONSE 1, a master transcription factor controlling DNA damage response in Arabidopsis. Plant J. **94**:439–453.

Őszi, E., Papdi, C., Mohammed, B., Petkó-Szandtner, A., Vaskó-Leviczky, T., Molnár, E., Galvan-Ampudia, C., Khan, S., Juez, E.L., Horváth, B., et al. (2020). E2FB interacts with RETINOBLASTOMA RELATED and regulates cell proliferation during leaf development. Plant Physiol. **182**:518–533.

Pedroza-García, J.A., Mazubert, C., Del Olmo, I., Bourge, M., Domenichini, S., Bounon, R., Tariq, Z., Delannoy, E., Piñeiro, M., Jarillo, J.A., et al. (2017). Function of the plant DNA Polymerase epsilon in replicative stress sensing, a genetic analysis. Plant Physiol. **173**:1735–1749.

Pedroza-Garcia, J.A., Xiang, Y., and De Veylder, L. (2022). Cell cycle checkpoint control in response to DNA damage by environmental stresses. Plant J. **109**:490–507.

Pennycook, B.R., Vesela, E., Peripolli, S., Singh, T., Barr, A.R., Bertoli, C., and de Bruin, R.A.M. (2020). E2F-dependent transcription determines replication capacity and S phase length. Nat. Commun. **11**:3503.

Preuss, S.B., and Britt, A.B. (2003). A DNA-damage-induced cell cycle checkpoint in Arabidopsis. Genetics **164**:323–334.

Saldivar, J.C., Cortez, D., and Cimprich, K.A. (2017). The essential kinase ATR: ensuring faithful duplication of a challenging genome. Nat. Rev. Mol. Cell Biol. **18**:622–636.

Sjogren, C.A., Bolaris, S.C., and Larsen, P.B. (2015). Aluminum-Dependent Terminal Differentiation of the Arabidopsis Root Tip Is Mediated through an ATR-ALT2-and SOG1-Regulated Transcriptional Response. Plant Cell **27**:2501–2515.

Sozzani, R., Maggio, C., Varotto, S., Canova, S., Bergounioux, C., Albani, D., and Cella, R. (2006). Interplay between Arabidopsis activating factors E2Fb and E2Fa in cell cycle progression and development. Plant Physiol. **140**:1355–1366.

Sweeney, P.R., Britt, A.B., and Culligan, K.M. (2009). The Arabidopsis ATRIP ortholog is required for a programmed response to replication inhibitors. Plant J. **60**:518–526.

Vandepoele, K., Raes, J., De Veylder, L., Rouzé, P., Rombauts, S., and Inzé, D. (2002). Genome-wide analysis of core cell cycle genes in Arabidopsis. Plant Cell **14**:903–916.

Vandepoele, K., Vlieghe, K., Florquin, K., Hennig, L., Beemster, G.T.S., Gruissem, W., Van de Peer, Y., Inzé, D., and De Veylder, L. (2005). Genome-wide identification of potential plant E2F target genes. Plant Physiol. **139**:316–328.

Verkest, A., Abeel, T., Heyndrickx, K.S., Van Leene, J., Lanz, C., Van De Slijke, E., De Winne, N., Eeckhout, D., Persiau, G., Van Breusegem, F., et al. (2014). A Generic Tool for Transcription Factor Target Gene Discovery in Arabidopsis Cell Suspension Cultures Based on Tandem Chromatin Affinity Purification. Plant Physiol. **164**:1122–1133.

Vlieghe, K., Vuylsteke, M., Florquin, K., Rombauts, S., Maes, S., Ormenese, S., Van Hummelen, P., Van de Peer, Y., Inze, D., and De Veylder, L. (2003). Microarray analysis of E2Fa-DPa-overexpressing plants uncovers a cross-talking genetic network between DNA replication and nitrogen assimilation. J. Cell Sci. **116**:4249–4259.

Yao, X., Yang, H., Zhu, Y., Xue, J., Wang, T., Song, T., Yang, Z., and Wang, S. (2018). The canonical E2Fs are required for germline development in Arabidopsis. Front. Plant Sci. **9**:638.

Yin, H., Zhang, X., Liu, J., Wang, Y., He, J., Yang, T., Hong, X., Yang, Q., and Gong, Z. (2009). Epigenetic regulation, somatic homologous recombination, and abscisic acid signaling are influenced by DNA polymerase epsilon mutation in Arabidopsis. Plant Cell **21**:386–402.

Yoshiyama, K., Conklin, P.A., Huefner, N.D., and Britt, A.B. (2009). Suppressor of gamma response 1 (SOG1) encodes a putative transcription factor governing multiple responses to DNA damage. Proc. Natl. Acad. Sci. USA **106**:12843–12848.